Journal of Applied Polymer Science

Complexation of macroporous amphoteric cryogels based on *N*,*N*-dimethylaminoethyl methacrylate and methacrylic acid with dyes, surfactant, and protein

Sarkyt E. Kudaibergenov,[1,2] Gulnur S. Tatykhanova,[1,2] Alexey N. Klivenko[3]

[1]Laboratory of Engineering Profile, Kazakh National Technical Research University n/a K.I. Satpayev, Satpayev Str. 22, Almaty 050013, Republic of Kazakhstan

[2]Institute of Polymer Materials and Technology, Satpayev Str. 22, Almaty 050013, Republic of Kazakhstan

[3]al-Farabi Kazakh National University, al-Farabi Av. 71, Almaty 050040, Republic of Kazakhstan

Correspondence to: S. Kudaibergenov (E-mail: skudai@mail.ru)

ABSTRACT: Macroporous amphoteric cryogels based on *N*,*N*-dimethylaminoethylmethacrylate and methacrylic acid p(DMAEM-*co*-MAA) crosslinked by *N*,*N*′-methylenebisacrylamide (MBAA) were synthesized by radical copolymerization of monomer mixtures in cryoconditions. The structure and morphology of cryogels were evaluated by FTIR and SEM. Cryogels exhibited interconnected porous structure with pore size ranging from 40 to 80 μm, which depended on their crosslinking degree. The value of the isoelectric point (IEP) of equimolar amphoteric cryogel determined from the water flux was equal to 4.4, while the IEP of cryogel with the excess of DMAEM units was equal to 7.1. The mechanical strength of equimolar amphoteric cryogels increases with increasing amount of crosslinking agent. The complexation ability of amphoteric cryogels with respect to surfactant, dyes, and protein was demonstrated. The adsorption isotherms with respect to anionic surfactant—sodium dodecylbenzene sulfonate (SDBS) and protein—lysozyme correspond to Langmuir equation, while adsorption isotherms of anionic and cationic dyes—methylene blue (MB) and methyl orange (MO) are well described by Freundlich equation. It was found that the binding ability of p(DMAEM-*co*-MAA) with respect to various low- and high-molecular weight compounds changes in the following order: SDBS > lysozyme ≫ MO > MB. The preferential adsorption of MB from the mixture of protein and MB was shown. The quantitative release of protein, surfactant and dye molecules from the matrix of cryogels takes place at the IEP of cryogel. © 2016 Wiley Periodicals, Inc. J. Appl. Polym. Sci. **2016**, *133*, 43784.

KEYWORDS: complexation; macroporous amphoteric cryogels; polymer gels

Received 16 May 2015; accepted 12 April 2016
DOI: 10.1002/app.43784

INTRODUCTION

Amphoteric nanogels[1] and microgels[2,3] have attracted significant attention in the last few years. The state-of the-art of amphoteric nanogel, microgel, and macrogel in light of their stimuli-responsive behavior and potential applications in nanotechnology, biotechnology, and medicine was recently reviewed.[4] The fundamental and applied aspects of nanogel and microgel systems together with recent developments in the synthesis, characterization, and application were outlined in review article.[5] Morphological, structural, and adsorption properties of cryogels were reviewed by authors.[6]

Structure, morphology, conformational, and volume-phase behavior of amphoteric nanogels,[7] and microgels[8–11] of p(DMAEM-*co*-MAA)[12] were evaluated. Uptake and release of surfactants from polyampholyte microgel particles was studied by authors.[8] It was concluded that depending on the surfactant type and the pH the electrostatic interactions, H-bonding, and hydrophobic bonding are realized. Polyampholyte nanocomposite hydrogels of AA, 2-(diethylamino)ethyl methacrylate (DEAEM) and montmorillonite were used for the removal of indigo carmine from textile aqueous effluents.[13] The adsorption of some textile dyes onto crosslinked poly(*N*-vinylpyrrolidone) was studied by Sahiner *et al.*[14] The micro- and macrogels based on quaternized poly(4-vinylpyridine)[15] as well as superporous poly((3-acrylamidopropyl)trimethylammonium chloride) cryogels[16] exhibited the high effectiveness in removal of cyanide and arsenate ions from aquatic environments. Poly(acrylamide) cryogel modified by amidoximation and in combination with nanoparticles of Cu, Ni and Co were used as superporous catalytic reactors in decontamination of toxic phenol compounds and some dyes from the wastewaters.[17] A macroporous amphoteric polymer based on N-[3-(dimethylamino)propyl]methacrylate and MAA was tailored in the presence of a pore-forming

agent ($CaCO_3$) and used as a template for bovine serum albumin and lysozyme.[18] Dual temperature/pH-sensitive polyampholyte gels of *N*,*N*-dimethylaminopropylacrylamide (DMAPAA) and AA were used as adsorbents and carriers with respect to bovine serum albumin (BSA).[19] The BSA adsorption was investigated as a function of MBAA concentration and temperature, and was discussed in terms of the difference in the sizes of BSA molecules and gel network. Deng *et al.*[7] studied the drug release behavior of polyampholyte nanogels using water-soluble chitosan as a model drug. Amphoteric hydrogel synthesized by gamma radiation-induced copolymerization of MAA and DMAEM in aqueous solution can be utilized for oral delivery of insulin.[20]

Comprehensive information on the structure, properties and application of cryogels in biotechnology and biomedicine and the pioneering articles devoted to cryogels can be found in a review[21] and fundamental book.[22]

Literature survey reveals that the most studied superporous cryogels for immobilization of metal nanoparticles exhibit anionic or cationic character.[23] Superporous cryogels of poly(acrylic acid),[24] poly(4-vinylpyridine),[25] and poly(2-acrylamido-2-methyl-1-propansulfonic acid)[26] and their templated metal nanoparticle composites were used in hydrogen generation from the hydrolysis of $NaBH_4$ and hydrogenation of 4-nitrophenol. Recently,[27] betaine type microgel based on poly2-(methacryloyloxy) ethyl]dimethyl(3-sulfopropyl)ammoniumhydroxide was used as a template for the *in situ* synthesis of Ni nanoparticles and as catalysts for hydrogenation of nitrogroup containing substrates—4-nitrophenol, 2-nitrophenol, and 4-nitroaniline.

In spite of advances in studying of nonionic, anionic and cationic nanogel, microgel, and macrogel to our knowledge there is very limited information on macroporous amphoteric gels themselves[28,29] and their complexation with various low- and high-molecular weight compounds.

In the present communication, we report for the first time (i) the preparation protocol and characterization of amphoteric cryogels based on p(DMAEM-*co*-MAA); (ii) the complexation ability of cryogels with respect to surfactant, dye molecules and protein; (iii) the release of adsorbed substances at the IEP of amphoteric cryogels.

EXPERIMENTAL

Materials

Monomers, catalyst and initiator—MAA(99% purity), DMAEM, (99% purity), *N*,*N*,*N*′,*N*′-tetramethylethylenediamine (TMED, 99% purity), ammonium persulfate (APS, 99% purity), and crosslinking agent *N*,*N*′-methylenbisacrylamide (MBAA, 99% purity) were purchased from Sigma-Aldrich Chemical, Milwaukee, WI, and used without further purification. Low-molecular weight substances, such as methylene blue (MB), methyl orange (MO), sodium dodecylbenzene sulfonate (SDBS), and lysozyme were purchased from AppliChem GmbH, Germany, and used without additional purification. The reason for choosing MB, MO, SDBS, and lysozyme for adsorption experiments is that the selected substances are easily detected spectrophotometrically in UV–Vis spectral regions.

Table I. Amount of DMAEM, MAA, and MBAA in the Feed Used for Synthesis of Cryogels

Initial monomer feed					
mg			mol %		
DMAEM	MAA	MBAA	DMAEM	MAA	MBAA
626	343	31	50	50	2.5
608	333	60	50	50	5
573	314	113	50	50	10
701	256	43	63	37	2.5

Methods

Absorption spectra were recorded with UV–Vis spectrophotometer (Specord 210 plus BU, Germany) at room temperature. FTIR spectra were recorded on a Cary 660 FTIR (Agilent, USA) in KBr pellets. Scanning electron microscopy (SEM) image was recorded using a high-resolution SEM (Zeiss Merlin High-Resolution SEM). The specimens were cutted, freeze-dried, and carbon-coated using Sputter-coater. Mechanical testing of cylindrical cryogel samples was performed using texture analyzer TA.XT plus, Stable Micro Systems (UK) as described in Ref. 30.

Synthesis of Amphoteric Cryogels

Mixture of MAA (343 mg or 4 mmol), DMAEM (626 mg or 4 mmol), MBAA (31 mg or 0.2 mmol) corresponding to the molar ratio of monomers MAA:DMAEM = 50:50 mol %/mol % was dissolved in 9 mL of deionized water, bubbled with nitrogen during 10 min and degassed under vacuum for about 5 min to eliminate dissolved oxygen. After addition of 10 μL of TMED the solution was cooled in an ice bath for 5 min. Then 0.1 mL of aqueous solution of APS (10 wt %) preliminary cooled in an ice bath for 5 min was added and the reaction mixture was stirred for 5 min. The total volume of reaction mixture was divided into 10 parts and each part containing 1 mL of reaction mixture was placed into the 10 glass cylinder with diameter 5 mm with closed outlet at the bottom. The solution in glass cylinder was frozen at −12 °C followed by cryopolymerization on cryothermostate LaudaProline RP 845 (Germany) during 48 h. After completion of the reaction the sample was thawed at room temperature. The prepared cryogel sample was washed thoroughly with distilled water every 2–3 h during several days then successively washed with 25, 50, 75, and 96% ethanol to dehydrate then it was dried in air and finally in vacuum oven to constant mass at room temperature. The amount of monomers in the feed mixture (in mg and mol %) used for the synthesis of cryogels is given in Table I.

Thus, a series of amphoteric cryogels crosslinked by 2.5, 5, and 10 mol % of MBAA were synthesized (Figure 1).

Swelling Experiments. The swelling capacity of cryogel samples as a function of pH was evaluated from the height measurements. For this dry gel sample with diameter 5 mm and height 8 mm was placed into a glass tube with diameter 7 mm. After passing of 100 mL of aqueous solutions through a gel sample with desired pH, that was adjusted by addition of 0.1 *N* HCl or KOH to distilled water to avoid the influence of buffer on

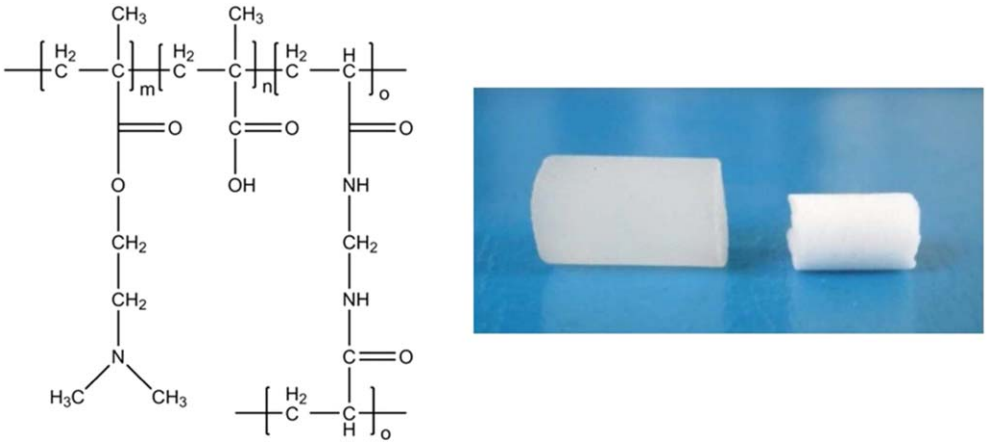

Figure 1. Structural units of amphoteric cryogels derived from DMAEM and MAA (left), image of dry and swollen in water cryogel samples (right). [Color figure can be viewed in the online issue, which is available at wileyonlinelibrary.com.]

swelling behavior, its height was accurately measured.[21,22] Swelling experiments were repeated three times with experimental error not exceeded ± 5%. The ratio of L_s/L_0 (where L_s is the height of swollen gel, L_0 is the height of dry gel) on time was plotted. The flow rate of water passing through the cryogel samples was measured at the constant hydrostatic pressure equal to 100 cm of water column corresponding to a pressure of ca. 0.01 MPa as described previously.[18] Measurements were repeated three times and the values averaged. The swelling rate p(DMAEM-*co*-MAA) cryogels in water is very fast and completed during 15 s (Figure 2). As expected increasing of crosslinking degree retards water absorption. In this connection, the flow rate experiments and adsorption of dyes, surfactant, and protein were carried out with cryogel samples crosslinked by 2.5 mol % MBAA.

Mechanical Testing of Equimolar p(DMAEM-*co*-MAA) Cryogels. The cylindrical shape cryogel samples with height 9.5–10 mm and contact area 78 mm^2 were fixed on the test table and compressed by the upper load cylinder-probe (P/10) at a test speed 0.1 mm/s using compression mode at room temperature. The force target mode was set up during all experiments. The Young modulus were determined from the initial parts of the stress/strain curves. All samples were tested three times and the results were averaged.

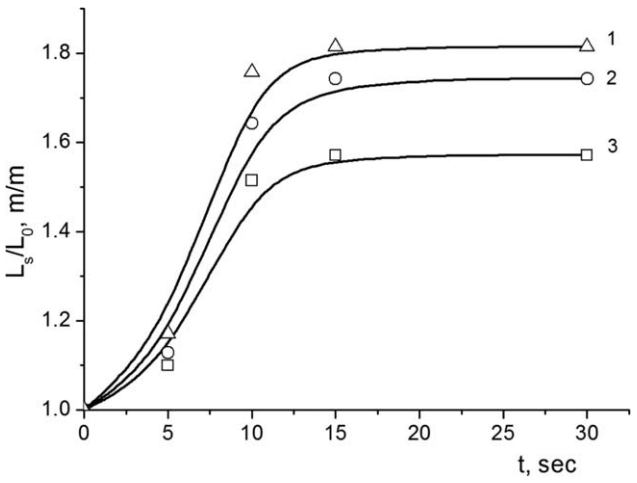

Figure 2. Time-dependent swelling of equimolar p(DMAEM-*co*-MAA) cryogels crosslinked by 2.5 (1), 5 (2), and 10 mol % (3) of MBAA.

Adsorption Experiments. All adsorption experiments were carried out with the amphoteric cryogel having the IEP of 7.1 at room temperature. The adsorption of lysozyme and MB was carried out in buffer solution at pH 9.5 while the SDBS and MO were adsorbed in buffer solution at pH 5.3. At these conditions, the hydrogel matrix and interacting components are oppositely charged and provide the maximal electrostatic interactions.

Adsorption of MB, MO, Lysozyme, and SDBS by p(DMAEM-*co*-MAA) Cryogel. A 20 mL aqueous solution of MB (or MO) containing 100, 200, 300, 400, and 500 mg L^{-1} dye was passed through 20 mg cryogel sample at pH 5.3 (for MO) and pH 9.5 (for MB) adjusted by acetate and phosphate buffers. The initial and final concentrations of MB (or MO) were determined spectrophotometrically at maximum absorbance region of MB (λ_{max} = 668 nm) and MO (λ_{max} = 505 nm). The same adsorption condition was selected also for lysozyme in buffer solution at pH 9.5. The amount of adsorbed lysozyme was determined at 275 nm. In case of surfactant adsorption, the concentration of SDBS varied in the range of 2–6 mmol L^{-1}. The initial and final concentrations of SDBS were determined at λ_{max} = 262 nm.

Adsorption of the Mixture of Lysozyme, SDBS, MB, and MO by p(DMAEM-*co*-MAA) Cryogel. To study the adsorption ability of p(DMAEM-*co*-MAA) with respect to the mixture of lysozyme and MB, the following experiments were carried out. At first, the cryogel specimen (m = 20 mg) was immersed into buffer solution with pH 9.5 overnight. After 20 mL aqueous solution containing 500 mg L^{-1} of lysozyme and 500 mg L^{-1} of MB at pH 9.5 was passed through cryogel. Adsorption spectra of solution passed through cryogel sample were measured continuously at the interval of wavelengths from 200 to 700 nm. Similar experiment was carried out for the mixture of MO and SDBS in buffer solution with pH 5.3. The initial

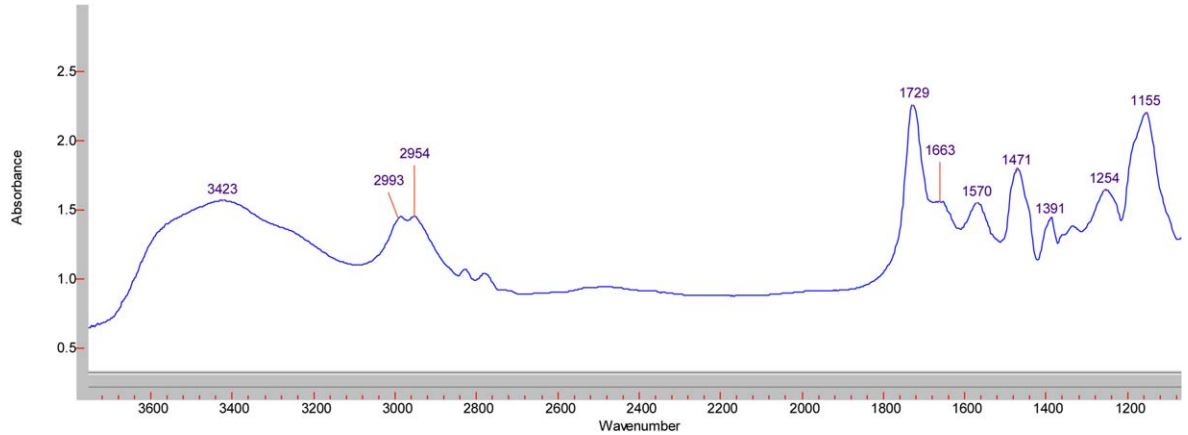

Figure 3. FTIR spectrum of p(DMAEM-*co*-MAA) cryogel. [Color figure can be viewed in the online issue, which is available at wileyonlinelibrary.com.]

concentrations of MO and SDBS passed through the cryogel specimen were equal to 500 mg L^{-1} and 5×10^{-3} mol L^{-1}, respectively. The initial and final concentrations of SDBS and MO were determined at λ_{max} = 262 and 668 nm.

Experiments on Release of SDBS, MO, MB, and Lysozyme from the Matrix of p(DMAEM-*co*-MAA)

Amphoteric cryogel samples (m = 20 mg) preliminary loaded separately with SDBS, MO, MB, and lysozyme was washed with 20 mL of buffer solutions at the same values of pH that were selected for adsorption (pH 5.3 or 9.5). In another series of experiments the cryogel samples were washed with buffer solution corresponding to the IEP of amphoteric cryogel (pH_{IEP} = 7.1). The concentrations of substances were measured as described above. The amount of released protein (surfactant and dyes) from cryogel matrix was calculated using the formulae: $W = \frac{m_{desorb}}{m_{adsorb}} \times 100\%$ (where m_{adsorb} is the amount of adsorbed protein (surfactant and dyes), m_{desorb} is the amount of desorbed protein (surfactant and dyes).

RESULTS AND DISCUSSION

Characterization of p(DMAEM-*co*-MAA) Cryogels

FTIR spectrum of amphoteric cryogel shows the characteristic bands of δOH (3423 cm^{-1}), νCH (2954 cm^{-1}), νC=O (1729 cm^{-1}), ν_{sym} COO^- (1663 cm^{-1}), ν_{asym} COO^- (1570 cm^{-1}), δCH (1471, 1391 cm^{-1}), νCOC (1155 cm^{-1}) groups (Figure 3).

Coexistence of $-COO^-$ and $-N(CH_3)_2H^+$ is due to partial transfer of protons from carboxylic groups to tertiary amine moieties. According to SEM images the pore sizes of cryogels decreasewith increasing of the crosslinking degree (Figure 4). The average pore size of p(DMAEM-*co*-MAA) samples is varied from 40 to 80 μm.

Mechanical Characteristics of p(DMAEM-*co*-MAA) Cryogels

As seen from Figure 5, the Young modulus of p(DMAEM-*co*-MAA) cryogels linearly increases with increasing the concentration of MBAA. It means that increasing the concentration of crosslinker strengthens the mechanical properties of cryogels.

Determination of the Composition of Amphoteric Cryogels by Adsorption of Dye Molecules

The composition of p(DMAEM-*co*-MAA) cryogel synthesized at equimolar ratio of acidic and basic monomers was determined by the procedure described in Ref. 31. Taking into account that the tertiary amine groups of cryogel will bind the sulfonate groups of MO while the carboxylic groups of cryogel will interact with tertiary amine groups of MB the residual amounts of dye molecules in eluate were determined. To achieve the complete binding of dyes to cryogels, pH of the solution was kept at

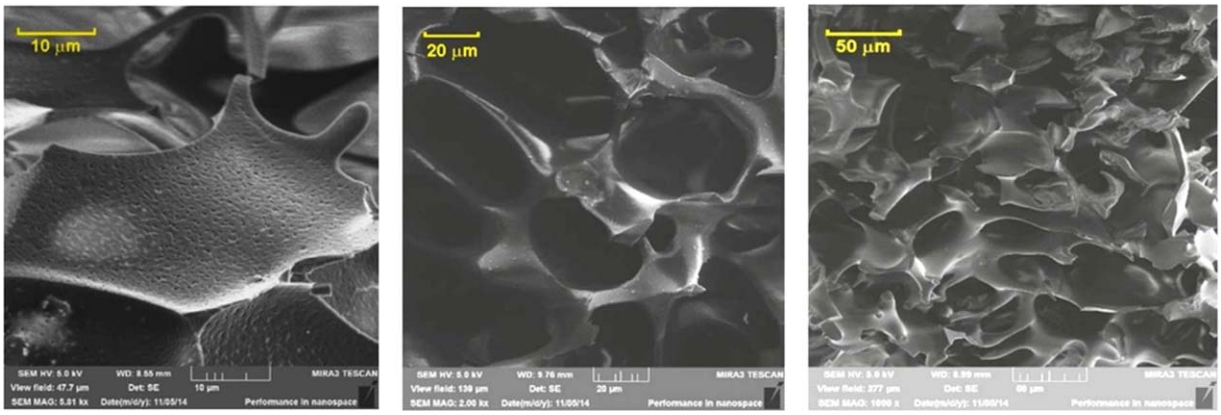

Figure 4. High-resolution SEM images of equimolar p(DMAEM-*co*-MAA) cryogel. [Color figure can be viewed in the online issue, which is available at wileyonlinelibrary.com.]

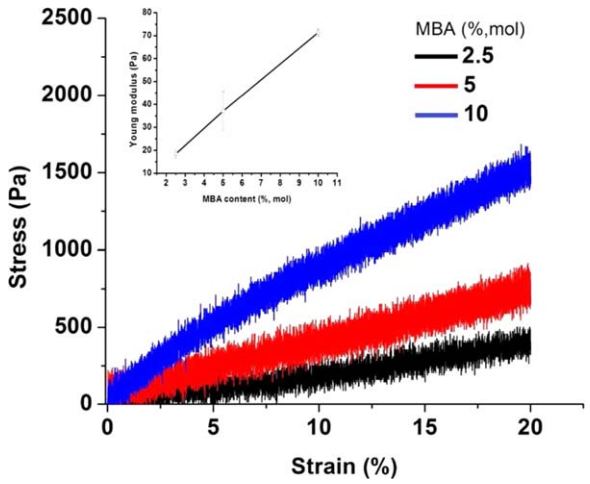

Figure 5. Stress–strain curves of p(DMAEM-*co*-MAA) cryogels at the concentration of MBAA 2.5 (1), 5 (2), and 10 mol % (3). Inset is the dependence of Young modulus on the content of MBAA. [Color figure can be viewed in the online issue, which is available at wileyonlinelibrary.com.]

5.3 in case of MO and pH = 9.5 in case of MB. However, in these experiments additional physical adsorption of dyes or retaining of dye molecules within cryogel pores was not taken into account. As seen from Figure 6 the cryogel samples have intensive color in solutions of MB and MO due to uptake of dye molecules via electrostatic attractions between functional groups of interacting components, while poly(acrylamide) cryogel not containing the charged groups is not able to absorb both MB and MO. The electrostatic nature of binding is confirmed by the fact that dye molecules are fully desorbed from the amphoteric cryogel volume into outer solution at the ionic strength of the solution $\mu = 0.1$ *M* KCl. Shielding of the positive or negative charges of amphoteric macromolecules by low-molecular weight anions or cations is responsible for detachment of ionic dyes. The composition of amphoteric cryogel found from the optical differences of dyes before and after immersion of cryogel samples to MB and MO solutions was equimolar and equal to 49.84 mol % of COOH groups and to 50.16 mol % of —$N(CH_3)_2$ groups. The composition of another sample synthesized at the excess of DMAEM in the monomer feed was equal to 37 mol % of —COOH and 63 mol % of —$N(CH_3)_2$ groups. It should be mentioned that this specific cryogel sample was used for adsorption experiments.

Determination of the IEP of Amphoteric Cryogel by Flow-Rate Experiments

One of the specific features of linear and crosslinked polyampholytes is the existence of so-called isoelectric points (IEPs)

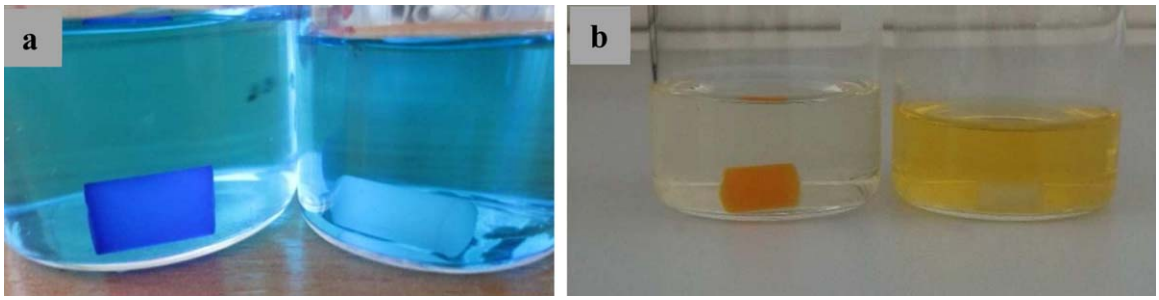

Figure 6. p(DMAEM-*co*-MAA) (left) and PAAm (right) cryogel samples immersed into aqueous solutions of MB (a) and MO (b). [Color figure can be viewed in the online issue, which is available at wileyonlinelibrary.com.]

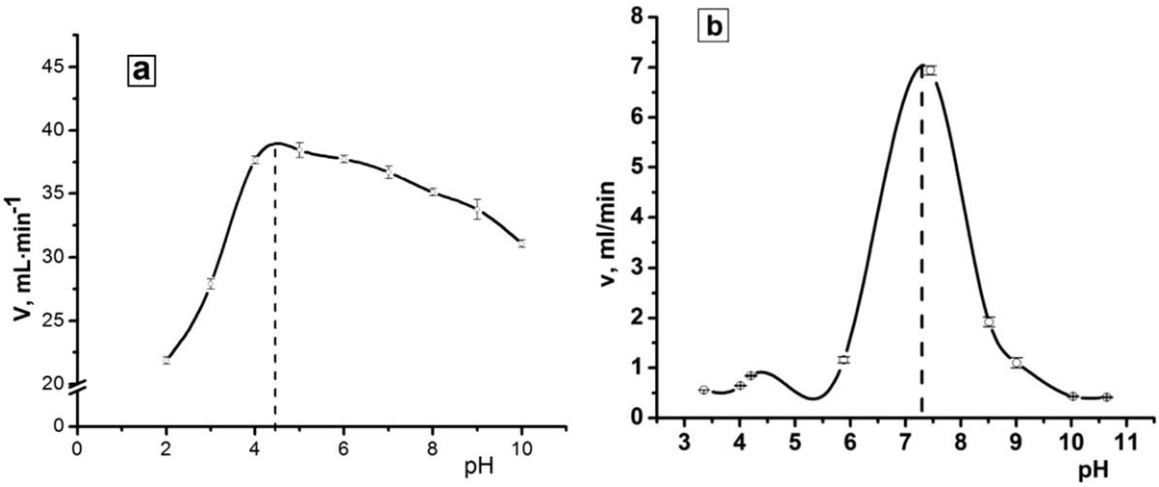

Figure 7. The pH dependent changes in the flow rate of water through p(DMAEM-*co*-MAA) cryogels. The compositions of amphoteric cryogels [DMAEM]:[MAA] are equal to 50.16:49.84 mol % (a) and 63:37 mol % (b). The dotted lines show the position of the IEP.

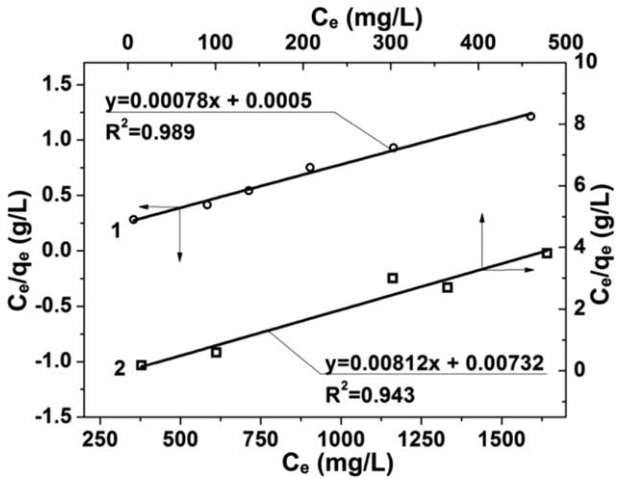

Figure 8. Langmuir isotherms of adsorption of SDBS (1) and lysozyme (2).

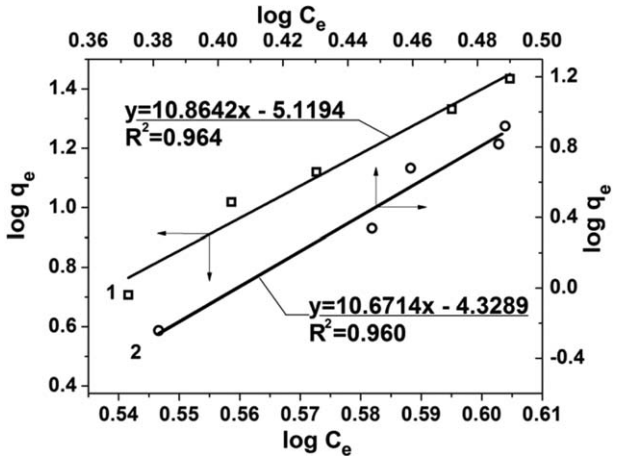

Figure 9. Freundlich isotherms of adsorption for MO (1) and MB (2).

where intra- and intermolecular attractions of opposite fixed charges lead to pseudoneutral behavior and compact structure of amphoteric macromolecules.[32,33] The IEPs of p(DMAEM-*co*-MAA) cryogel was determined by the measurement of the rate of water flow through the sample as a function of pH. As seen from Figure 7, the maximal values of water flow rate correspond to 4.4 and 7.1 that are accepted as IEPs because any deviation from the IEPs due to excess of the positive or negative charges leads to swelling and accumulating of water molecules around the charged groups. At the IEP the positive and negative charges are mutually compensated, macromolecular chains become more hydrophobic repelling water molecules from the inner, surface and outer parts of cryogel.

Adsorption Isotherms. The adsorption isotherms of surfactant (SDBS), dyes (MB and MO), and protein (lysozyme) were plotted using Langmuir and Freundlich equations as described in Ref. 16. Langmuir monomolecular adsorption model is based on equation:

$$C_e/q_e = C_e/q_m + 1/q_m \times K_L \quad (1)$$

where C_e concentration of substance at equilibrium mg L^{-1}, q_e equilibrium adsorption capacity mg g^{-1}, q_m maximal adsorption capacity, K_L Langmuir adsorption equilibrium constant, L mg^{-1}.

Langmuir model provides the determination of the maximal adsorption capacity. As seen from Figure 8 and Table II the Langmuir model gives the $R^2 = 0.943$ and 0.989 for adsorption of lysozyme and SDBS, respectively. The experimental value of q_m for lysozyme (123.04 mg g^{-1}) coincides well with theoretical, while the q_m for SDBS (1313 mg g^{-1}) is higher than the theoretical value. The latter is probably due to hydrophobic interactions between adsorbed and nonadsorbed SDBS within macropores of cryogel.

In contrast to lysozyme and SDBS that are correctly described by Langmuir model, the adsorption of dye molecules corresponds to the empirical Freundlich equations (2)(3):

$$q_e = K_F \times C_e^n \quad (2)$$

$$\log\ q_e = \log\ K_F + 1/n \times \log\ C_e \quad (3)$$

where n and K_F is constants of Freundlich isotherm, C_e concentration of substance at equilibrium state, mg L^{-1}, q_e equilibrium adsorption capacity, mg g^{-1}.

The values of Freundlich isotherms together with K_F and n are shown in Figure 9 and summarized in Table III.

As follows from the Freundlich equation (2) the adsorption capacity increases with increasing of K_F and n. The values of q_m at different pH are summarized in Table IV.

Selectivity of Amphoteric Cryogel with Respect to the Mixture of Protein, Surfactant and Dye

As described above the adsorption of the mixture of MO and SDBS by p(DMAEM-*co*-MAA) was carried out at pH 5.3, while the mixture of lysozyme and MB was adsorbed at pH 9.5.

As seen from Figure 10(a), at pH 9.5 the p(DMAEM-*co*-MAA) adsorbs MB more effectively rather than lysozyme. Preferential adsorption of MB may be accounted for stronger electrostatic binding of the quaternary ammonium groups of MB (=N^+<) by carboxylate anions of cryogel than that of NH_3^+ groups of lysozyme. Also the greater hydrodynamic size of lysozyme can restrict the effective binding of protein molecules inside cryogel pores. At the same time, there is no substantial difference between the adsorption capacity of SDBS or MO with respect to p(DMAEM-*co*-MAA) [Figure 10(b)]. Probably the positively

Table II. Langmuir Isotherm Constants

Substance	K_L, L mg^{-1}	q_m, mg g^{-1}	R^2
Lysozyme	1.11	123.15	0.943
SDBS	1.56	1282.05	0.989

Table III. Freundlich Isotherm Constants

Substance	K_F, L mg^{-1}	n	R^2
MO	7.6×10^{-6}	0.092	0.964
MB	4.7×10^{-5}	0.094	0.960

Table IV. Adsorption of Dyes, Surfactant, and Protein by Amphoteric Cryogel

Substances	q_m, mg g^{-1}	pH of adsorption
Lysozyme	123	9.5
MB	8.3	9.5
SDBS	1313	5.3
MO	27.1	5.3

According to adsorption isotherms the binding ability of p(DMAEM-*co*-MAA) changes in the following order: SDBS > lysozyme ≫ MO > MB.

charged amine groups of DMAEM do not discriminate the negatively charged sulfonate groups of SDBS and MO.

Release of Adsorbed Lysozyme, SDBS, MB, and MO at the IET of Cryogel

Earlier[34] the so-called "isoelectric effect" was established for linear polyampholytes, where the preliminary adsorbed at appropriate pH the low- and high molecular compounds such as proteins, metal ions, ionic dyes, and surfactants are released strictly at the IEP of amphoteric macromolecules. In this connection it was interesting to test the feasibility of such phenomenon for crosslinked amphoteric macroporous cryogels. Table V shows the maximal amount of adsorbed substances at pH 5.3 and 9.5.

The amount of MO and SDBS washed out at pH 5.3 is 5.5 and 6.7%, respectively. The amount of lysozyme and MB washed out at pH 9.5 is equal to 2 and 6%. The release of dye molecules, surfactant and protein at the IEP of amphoteric cryogel (pH_{IEP} = 7.1) reaches up to 98%. The profound release effect is realized for MB as visualized in Figure 11. Washing out of preliminary adsorbed MB by buffer solution at pH 9.5 leads to retaining of intensive color in cryogel sample while the pale color of supernatant confirms the minimal release of MB. Substantial discoloration of cryogel sample and high color of supernatant at pH 7.1 evidences the effective release of MB at the IEP of cryogel.

Table V. Adsorbed Amount of MB, MO, SDBS, and Lysozyme by p(DMAEM-*co*-MAA) at Different pH

Substance	Initial concentration, mg L^{-1}	q, mg g^{-1}	pH of adsorption
MO	500	0.14	5.3
SDBS	1700	19.2	
Lysozyme	500	1.75	9.5
MB	500	0.043	

The amount of MB, MO, lysozyme, and SDBS released at the IEP is given in Table VI.

Table VI. Release of MB, MO, Lysozyme, and SDBS from p(DMAEM-*co*-MAA) Cryogel at Different pH

	Release, mg/%		
	pH		
Substance	7.1	9.5	5.3
MB	0.04/94	0.003/6	—
MO	0.13/94.5	—	0.0076/5.5
Lysozyme	1.72/98	0.035/2	—
SDBS	17.9/93.2	—	1.3/6.7

Release mechanism of low- and high molecular compounds at the IEP of amphoteric cryogel is explained by Figure 12. The p(DMAEM-*co*-MAA) is positively charged at pH 5.3 due to ionization of tertiary amine groups and negatively charged at pH 9.5 due to ionization of carboxylic groups while is electroneutral at the IEP (pH 7.1). At pH 9.5 the MO has the fixed positive charge (=N^+<), the lysozyme is also charged positively because its isoionic point (IIP) is equal to pH_{IIP} 10.7. Thus at pH 9.5 the negatively charged cryogel matrix binds both MB and lysozyme electrostatically. Whereas at pH 5.3 the positively charged cryogel matrix captures the negatively charged SDBS and MO

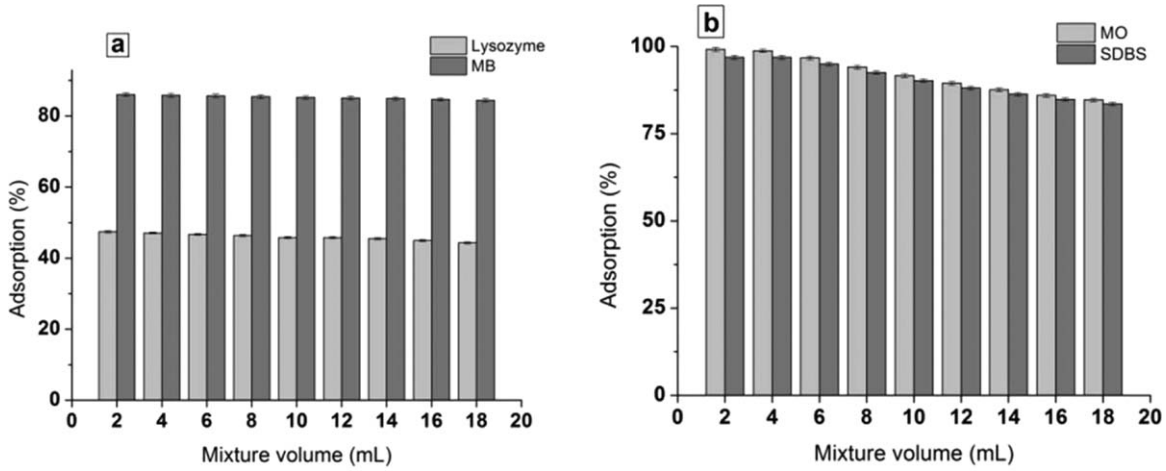

Figure 10. Adsorption of the mixture of lysozyme and MB (a) and the mixture of SDBS and MO (b).

Figure 11. Cryogel samples washed with buffer solution at pH 9.5 (a) and pH 7.1 (b). [Color figure can be viewed in the online issue, which is available at wileyonlinelibrary.com.]

through electrostatic interaction between the SO_3^- groups of MO and SDBS and $-N(CH_3)_2H^+$ moieties of cryogel.

At the IEP of amphoteric cryogel the cooperativity of intrachain interactions between the acidic and basic groups (formation of inner salt) within a cryogel matrix predominates those of interchain interactions between cryogel and protein, surfactant and dye molecules. In other words at the IEP of amphoteric cryogel the mutual electrostatic attraction between the positive and negative charges overcomes the electrostatic interaction between negatively charged cryogel and positively charged protein (or MB) resulting in a release of positively charged protein (or MB) from the cryogel matrix to the outer solution. The same mechanism is realized for positively charged cryogel and negatively charged SDBS and MO molecules at the IEP of amphoteric cryogel. Since the opposite charges of amphoteric cryogel neutralize each other more cooperatively and effectively at the IEP, a negligible amount of protein, surfactant and dye molecules retains within the pores of cryogel.

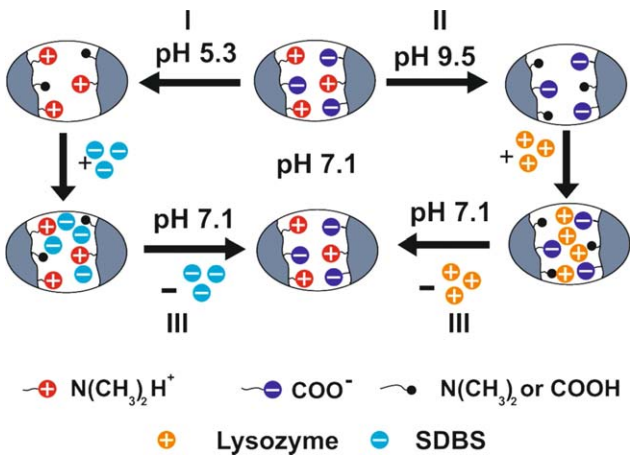

Figure 12. Schematic representation of adsorption of SDBS at pH 5.3 (route 1), lysozyme at pH 9.5 (route 2), and their release at pH 7.1 (IEP) (route 3). [Color figure can be viewed in the online issue, which is available at wileyonlinelibrary.com.]

CONCLUSIONS

Amphoteric cryogels of p(DMAEM-*co*-MAA) were synthesized by cryopolymerization technique. SEM images of cryogels show sponge-like porous structure composed of interconnected channels. Both pore size and water flux decreases with increasing crosslinking degree. The isoelectric points of p(DMAEM-*co*-MAA) cryogels found from the swelling measurements are equal to 4.4 and 7.1. The binding ability of p(DMAEM-*co*-MAA) cryogel with respect to protein, surfactant and dyes changes in the following order: SDBS > lysozyme ≫ MO > MB. The electrostatic forces are responsible for the complexation of abovementioned substances with amphoteric cryogels. The adsorption isotherms of SDBS and lysozyme correspond to Langmuir type while the adsorption of dyes is better described by Freundlich type. Preferential adsorption of MB from the mixture of lysozyme and MB is shown. Simultaneous adsorption of anionic surfactant and anionic dye by cryogel sample is observed for both SDBS and MO from their mixture. The isoelectric effect is realized at the IEP of amphoteric cryogel and the release of adsorbed substances falls within the range of 93–98%.

ACKNOWLEDGMENTS

Financial support from the Ministry of Education and Science of the Republic of Kazakhstan (1004/GF4 2015-2017) is greatly acknowledged. Authors thank Assistant Professor Nurxat Nuraje from Department of Chemical Engineering, Texas Tech University for high resolution SEM measurements. Proof reading of this manuscript by Prof. Vitaliy Khutoryanskiy at University of Reading, UK, is greatly acknowledged.

REFERENCES

1. Sankar, R. M.; Meera, K. M. S.; Samanta, D.; Jithendra, P.; Mandal, A. B.; Jaisankar, S. N. *Colloids Surf. B: Biointerfaces* **2013**, *112*, 120.
2. McCann, J.; Thaiboonrod, S.; Ulijn, R. V.; Saunders, B. R. *J. Colloid Interface Sci.* **2014**, *415*, 151.
3. Graham, N. B.; Cameron, A. *Pure Appl. Chem.* **1998**, *70*, 1271.
4. Kudaibergenov, S. E.; Nuraje, N.; Khutoryanskiy, V. V. *Soft Matter* **2012**, *8*, 9302.
5. Pich, A.; Richtering, W. In Polymer Science: A Comprehensive Reference; Möller, K. M., Ed.; Elsevier: Amsterdam, **2012**.
6. Gun'ko, V. M.; Savina, I. N.; Mikhalovsky, S. V. *Adv. Colloid Interface Sci.* **2013**, *187*, 1.
7. Deng, L.; Zhai, Y.; Guo, S.; Jin, F.; Xie, Z.; He, X.; Dong, A. *J. Nanoparticle Res.* **2009**, *11*, 365.
8. Bradley, M.; Vincent, B.; Burnett, G. *Colloid Polym. Sci.* **2009**, *287*, 345.

9. Christodoulakis, K. E.; Vamvakaki, M. *Langmuir* **2010**, *26*, 639.
10. Tan, B. H.; Tam, K. C. *Adv. Colloid Interface Sci.* **2008**, *136*, 25.
11. Tan, B. H.; Ravi, P.; Tam, K. C. *Macromol. Rapid Commun.* **2006**, *27*, 522.
12. Shen, Y.; Li, X.; Liu, H.; Shu, X.; Liu, M.; Zhang, L. *Gaofenzi Cailiao Kexue Yu Gongcheng/Polym. Mater. Sci. Eng.* **2011**, *27*, 139.
13. Dalaran, M.; Emik, S.; Guclu, G.; Iyim, T. B.; Ozgumus, S. *Desalination* **2011**, *279*, 170.
14. Ekici, S.; Isikver, Y.; Sahiner, N.; Saraydin, D. *Adsorp. Sci. Technol.* **2003**, *21*, 651.
15. Sahiner, N.; Ozay, O.; Aktas, N. *Water Air Soil Pollut.* **2013**, *224*, 1393.
16. Sahiner, N.; Demirci, S.; Sahiner, M.; Yilmaz, S.; Al-Lohedan, H. *J. Environ. Manage.* **2015**, *152*, 66.
17. Sahiner, N.; Seven, F.; Al-lohedan, H. *Water Air Soil Pollut.* **2015**, *226*, 122.
18. Huang, J. T.; Zhang, J.; Zhang, J. Q.; Zheng, S. H. *J. Appl. Polym. Sci.* **2005**, *95*, 358.
19. Kanazawa, R.; Sasaki, A.; Tokuyama, H. *Sep. Purif. Technol.* **2012**, *96*, 26.
20. Abou Taleb, M. F. *Int. J. Biol. Macromol.* **2013**, *62*, 341.
21. Lozinsky, V. I. *Russ. Chem. Rev.* **2002**, *71*, 489.
22. Mattiasson, B.; Kumar, A.; Galaev, I. Macroporous Polymers; CRC Press/Taylor & Francis: Boca Raton, **2010**, p 513.
23. Sahiner, N. *Prog. Polym. Sci.* **2013**, *38*, 1329.
24. Sahiner, N.; Seven, F. *Energy* **2014**, *71*, 170.
25. Sahiner, N.; Yildiz, S. *Fuel Process. Technol.* **2014**, *126*, 324.
26. Sahiner, N.; Seven, F. *RSC Adv.* **2014**, *4*, 23886.
27. Ajmal, M.; Siddiq, M.; Aktas, N.; Sahiner, N. *RSC Adv.* **2015**, *5*, 43873.
28. Tatykhanova, G. S.; Sadakbayeva, Z. K.; Berillo, D.; Galaev, I.; Abdullin, K. A.; Adilov, Z.; Kudaibergenov, S. E. *Macromol. Symp.* **2012**, *317–318*, 18.
29. Kudaibergenov, S.; Adilov, Z.; Berillo, D.; Tatykhanova, G.; Sadakbaeva, Z.; Abdullin, K.; Galaev, I. *Expr. Polym. Lett.* **2012**, *6*, 346.
30. Khutoryanskaya, O. V.; Mayeva, Z. A.; Mun, G. A.; Khutoryanskiy, V. V. *Biomacromolecules* **2008**, *9*, 3353.
31. Gaur, R. K.; Gupta, K. C. *Anal. Biochem.* **1989**, *180*, 253.
32. Kudaibergenov, S. E. Polyampholytes: Synthesis, Characterization, and Application; Kluwer Academic/Plenum Publishers: New York, **2002**.
33. Ciferri, A.; Kudaibergenov, S. *Macromol. Rapid Commun.* **2007**, *28*, 1953.
34. Kudaibergenov, S. E. In Encyclopedia of Polymer Science and Technology; John Wiley & Sons, Inc.: New York, **2002**.